

Electronic Supplementary Information

For

Lewis Base Mediated Dismutation of Trichlorosilane†‡

Amit Pratap Singh,^a Rajendra S. Ghadwal,^a Herbert W. Roesky,^{a,*} Julian J. Holstein,^a Birger Dittrich,^{a,*} Jean-Philippe Demers,^b Veniamin Chevelkov^b and Adam Lange^b

^a Institut für Anorganische Chemie, Universität Göttingen, Tammannstrasse 4, 37077 Göttingen, Germany

^b Max-Planck-Institut für Biophysikalische Chemie, Am Faßberg 11, D-37077 Göttingen, Germany

AUTHOR EMAIL ADDRESS hroesky@gwdg.de, bdittri@gwdg.de

Content:

S1. Experimental Section

S2. Solid state ²⁹Si NMR

S3. Single crystal X-ray analysis and DFT geometry optimizations

S3. References

S1. Experimental section:

All manipulations were performed in a dry and oxygen free atmosphere (N_2) using standard Schlenk-line techniques and inside a MBraun MB 150-GI glove box maintained at or below 1 ppm of O_2 and H_2O . All solvents were dried by a MBraun solvent purifying system prior to use. Abnormal N-heterocyclic carbene (aNHC) was synthesized by the reported procedures.^(S1) Other chemicals were purchased commercially and used as received. The 1H , ^{13}C , and ^{29}Si NMR spectra were recorded on a Bruker Avance DRX instrument (300 or 500 MHz, 1H Larmor frequency). The chemical shifts δ are given in ppm with tetramethylsilane as external standards. Elemental analyses were performed by the Analytisches Labor des Instituts für Anorganische Chemie der Universität Göttingen.

Synthesis of $(NHC)_2\cdot SiCl_2H_2$ (2). To a 100 mL toluene solution of NHC (17.25 g, 44.39 mmol) was condensed H_2SiCl_2 (2.24 g, 22.17 mmol) at $-78\text{ }^\circ C$ with constant stirring. The resulting white suspension was stirred overnight at room temperature. All the volatiles were removed under vacuum to afford off-white solid, which was washed with *n*-hexane (2x20 mL). Recrystallization from a toluene-*n*-hexane mixture (1:1) gave colorless crystals of **2** suitable for single crystal X-ray structural analysis (Yield 13 g, 67%). Elemental analysis (%) calcd for $C_{54}H_{74}Cl_2N_4Si$: C 73.85, H 8.49, N 6.38; found: C 73.81, H 8.43, N 6.33. 1H NMR (200 MHz, C_6D_6 , 25 $^\circ C$): δ 1.02 (d, $J = 5.98$ Hz, 24H, $CHMe_2$); 1.23 (d, $J = 5.88$ Hz, 24H, $CHMe_2$); 3.19 (m, 8H, $CHMe_2$); 5.58 (br, 2H, SiH); 6.30 (s, 4H, NCH), 7.06-7.25(m, 12H, C_6H_3) ppm. ^{13}C NMR (125 MHz, C_6D_6 , 25 $^\circ C$): δ 24.02, 24.63 ($CHMe_2$); 28.75 ($CHMe_2$); 122.24, 123.79, 129.40, 137.43 (C_6H_3); 146.42 (*ipso*- C_6H_3) ppm. ^{29}Si (1H - ^{29}Si HSQC) NMR (79 MHz, C_6D_6 , 25 $^\circ C$): δ – 225.2 ppm.

Synthesis of aNHC-SiCl₂H₂ (3). Compound **3** was synthesized by the reaction of aNHC (1.00 g, 1.85 mmol) in toluene with the addition of $HSiCl_3$ (0.38 mL, 3.88 mmol) at $-78\text{ }^\circ C$ under nitrogen atmosphere and stirred for 30 min. The mixture was then warmed to room temperature

and stirred during 6 h. All volatiles were removed under vacuum to afford a light yellow colored crude product. The crude product was washed with *n*-hexane (2 x 20 mL) to afford a colorless solid. The crude product was again dissolved in a minimum amount of toluene and filtered through the pad of Celite of a medium porosity frit. The filtrate was stored for three days at room temperature to give colorless crystalline **3** suitable for single crystal X-ray structural analysis (Yield 0.93 g, 78%). Mp = 280 °C (dec.). Elemental analysis (%) calcd for C₃₉H₄₆Cl₂N₂Si (641.79): C, 72.99; H, 7.22; N, 4.36. Found: C, 73.16; H, 7.34; N, 4.03. ¹H NMR (500 MHz, THF-*d*₈, TMS, 25 °C): δ 7.38–7.29 (m, 3H, CH_{ar}), 7.20–7.12 (m, 3H, CH_{ar}), 7.10–6.98 (m, 8H, CH_{ar}), 6.92–6.83 (m, 2H, CH_{ar}), 6.14 (s, 2H, Si-H), 3.24 (sept, 2H, Ar-CH(CH₃)₂), 2.60 (sept, 2H, Ar-CH(CH₃)₂), 1.44 (d, *J* = 6.8 Hz, 6 H, CH₃), 0.91 (d, *J* = 6.8 Hz, 6 H, CH₃), 0.88 (d, *J* = 6.8 Hz, 6 H, CH₃), 0.72 (d, *J* = 6.8 Hz, 6 H, CH₃) ppm. ¹³C NMR (500 MHz, THF-*d*₈, TMS, 25 °C): δ 145.8, 145.5, 141.4, 141.3, 140.3, 136.6, 134.4, 131.3, 130.2, 129.8, 129.4, 128.8, 128.5, 128.2, 126.3, 126.1, 124.4, 29.7 (CHCH₃), 29.4 (CHCH₃), 25.7(CH₃), 24.3 (CH₃), 23.9 (CH₃), 22.8 (CH₃) ppm. ²⁹Si NMR(500 MHz, THF-*d*₈, TMS, 25 °C): δ -118.20 (*J*_{Si-H} = 337 Hz) ppm. Compound **3** was also synthesized from a similar procedure as followed for compound **2**, by the reaction of aNHC (1.00 g, 1.85 mmol) in toluene with H₂SiCl₂ (0.18 g, 1.85 mmol) at -78 °C. Crude compound was purified by crystallization from a saturated toluene solution to gives colorless crystalline product (Yield 0.70 g, 59%).

Synthesis of aNHC·GeCl₂ (4). For the synthesis of compound **4**, the toluene solution of aNHC (1.00 g, 1.85 mmol) was treated with solid Cl₂Ge·dioxane (0.43 g, 1.85 mmol) under nitrogen atmosphere at -78 °C. The mixture was then warmed to room temperature and stirred for 10 h. All volatiles were removed under vacuum to afford a colorless crude product. The crude product was again dissolved in a minimum amount of toluene and filtered through a pad of Celite of a medium porosity frit. The filtrate was stored for two days at room temperature to give colorless crystalline **4** suitable for single crystal X-ray structural analysis (Yield 1.01 g, 80%). Mp = 265

°C (dec.). Elemental analysis (%) calcd for C₃₉H₄₄Cl₂GeN₂ (684.33): C, 68.45; H, 6.48; N, 4.09. Found: C, 68.73; H, 6.79; N, 4.05. ¹H NMR (500 MHz, THF-*d*₈, TMS, 25 °C): δ 7.61–7.57 (m, 3H, CH_{ar}), 7.53–7.44 (m, 3H, CH_{ar}), 7.39–7.20 (m, 8H, CH_{ar}), 7.16–7.01 (m, 2H, CH_{ar}), 2.91–2.62 (m, 4H, Ar-CH(CH₃)₂), 1.48 (d, *J* = 6.8 Hz, 6 H, CH₃), 1.03 (d, *J* = 6.8 Hz, 6 H, CH₃), 0.99 (d, *J* = 6.8 Hz, 6 H, CH₃), 0.93 (d, *J* = 6.8 Hz, 6 H, CH₃) ppm. ¹³C NMR (500 MHz, THF-*d*₈, TMS, 25 °C): δ 155.8, 140.4, 138.2, 135.4, 133.2, 130.1, 129.6, 125.2, 123.3, 120.1, 118.4, 115.4, 113.8, 110.2, 109.2, 106.3, 103.1, 101.4, 29.7 (CHCH₃), 29.5 (CHCH₃), 25.2(CH₃), 24.3 (CH₃), 24.1 (CH₃), 23.9 (CH₃) ppm.

S2. ²⁹Si Solid-state NMR

Solid-state NMR spectra were recorded at temperatures of 5–10 °C on a 9.4 T (400 MHz ¹H Larmor frequency) wide-bore instrument. Micro-crystals of compounds **2** and **3** were packed under inert atmosphere into 4.0-mm magic-angle spinning (MAS) rotors. ¹H-²⁹Si cross-polarization (CP) spectra were recorded at MAS frequencies of 1250 Hz and 7000 Hz (black spectra in Fig. S1). Proton decoupling was applied during acquisition using the SPINAL-64 sequence^(S2) with RF field amplitudes in the range of 62.5–83.3 kHz. Chemical shifts were calibrated using external 3-(trimethylsilyl)-propanoic acid, sodium salt (TMSP) as a reference for ²⁹Si.

The chemical shift anisotropies of ²⁹Si were extracted by comparison of spinning sideband intensities with the sideband pattern of simulated spectra (Figure S1). Simulated spectra were generated within the numerical simulation routine GAMMA^(S3) over a large range of possible anisotropy and asymmetry values. The ²⁹Si anisotropic chemical shift was considered as the relevant internal system Hamiltonian, and powder averaging involved 1154 crystallite orientations. Values for the principal components of the CSA tensor which minimize the peak intensity residual sum of squares were selected in a joint fit of both MAS frequency spectra

(Table S1), and were used to produce the back-calculated spectra (red spectra in Fig. S1). The presence of directly bonded protons was confirmed for both silicon atoms in **2** and **3** by recording ^1H - ^{29}Si cross-polarization build-up curves (Fig. S2) where contact times for CP were increased in the range 0–1.6 ms.

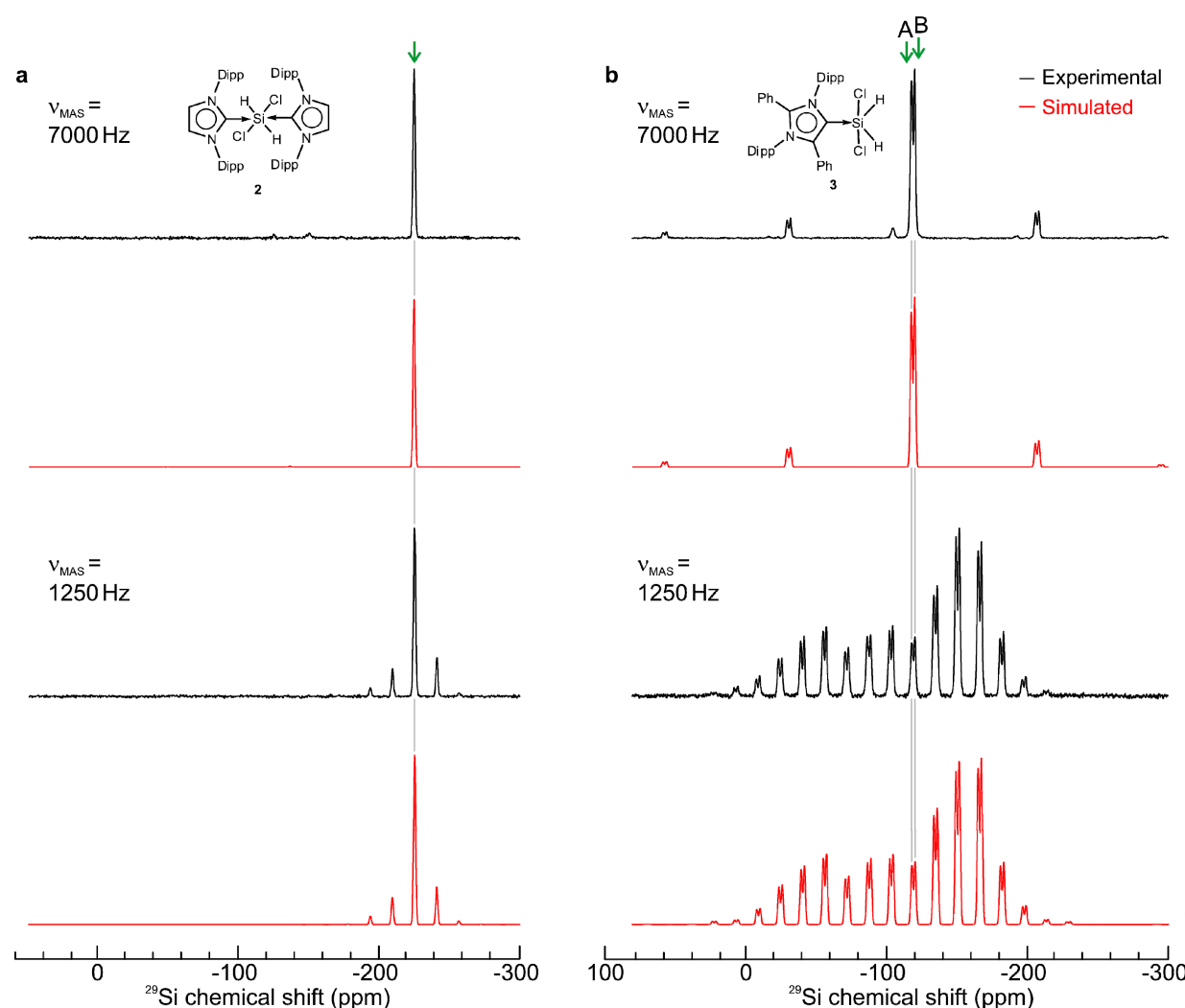


Fig. S1. ^{29}Si Cross-polarization spectra of (a) the 2:1 adduct $(\text{NHC})_2\cdot\text{SiCl}_2\text{H}_2$ compound **2** and (b) the abnormal 1:1 adduct $\text{aNHC}\cdot\text{SiCl}_2\text{H}_2$ compound **3**. Experimental spectra are presented in black and back-calculated spectra in red. The spectra were recorded at MAS frequencies of 7000 Hz (top panels) and 1250 Hz (bottom panels). Isotropic peaks are indicated by green arrows, at -225.2 ppm for **2** and at -118.0 ppm (site A) and -120.4 (site B) for **3**. The two sites have a frequency separation of 190 Hz. The high number of spinning sidebands and large breadth of the spectrum for the five coordinate adduct **3** is especially apparent at 1250 Hz MAS, reflecting the large anisotropy of the electronic environment at the Si nucleus. In contrast, spectra

of the six-coordinated 2:1 adduct **2** present fewer sidebands, as the inherent symmetry of the molecule results in a more isotropic electronic environment at the Si nucleus.

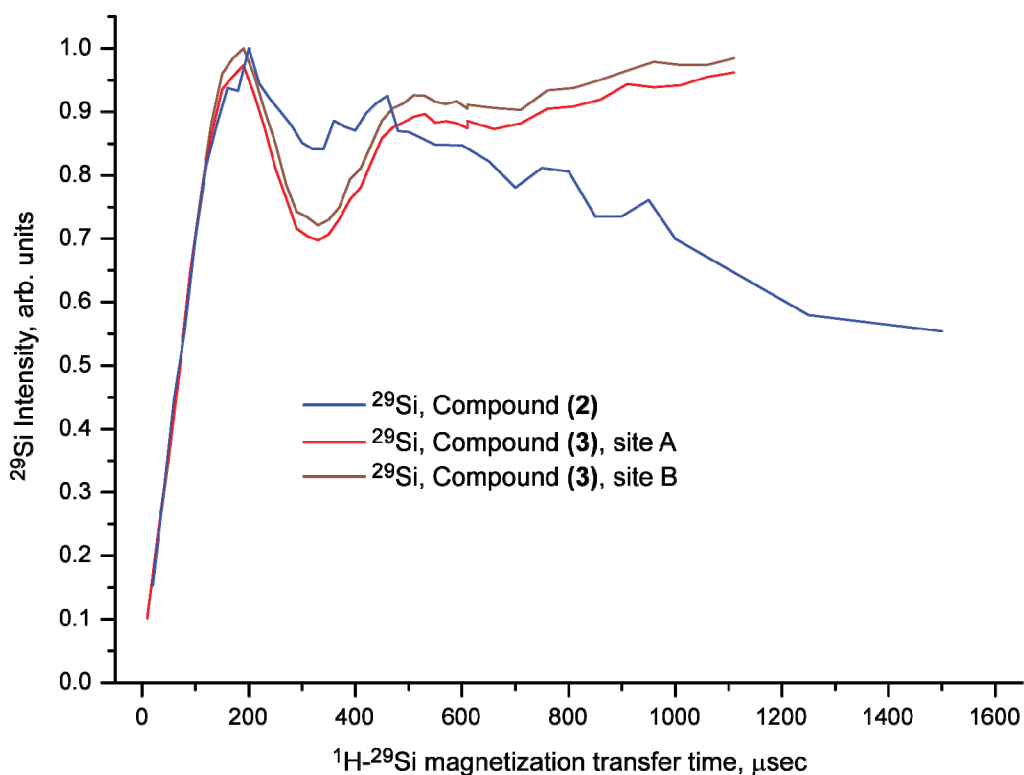


Fig. S2. Build-up curves of ^{29}Si signal intensity during ^{29}Si cross-polarization for compound **2** (blue) and compound **3**. (red, site A; dark red, site B). The first maxima in signal intensity are obtained at short CP contact times: 200 μs for **2** and 180 μs for **3**. This fast transfer brought about by strong dipolar couplings can only arise for short $^1\text{H}-^{29}\text{Si}$ inter-nuclear distances and constitutes a direct confirmation of the presence of protons directly bonded to silicon. In contrast, the magnetization transfer maximum is obtained at 2400 μs for TMSP in the same conditions (not shown), where no proton is directly bonded to the silicon atom.

Table S1. Chemical shift tensor parameters and optimum cross-polarization contact times

| Compound | τ_{CP} (μs) | δ_{iso} (ppm) | δ_{aniso} (ppm) | η_{asym} | δ_{xx} (ppm) | δ_{yy} (ppm) | δ_{zz} (ppm) |
|------------------|---|--------------------------------|----------------------------------|----------------------|-------------------------------|-------------------------------|-------------------------------|
| 2 (exp.) | 200 | -225.2 | +24 | 0.49 | -243.1 | -231.3 | -201.2 |
| 2 (theo.) | — | -185.4 | -26 | 0.88 | -161.4 | -183.9 | -210.9 |
| 3A (exp.) | 190 | -118.0 | +112 | 0.29 | -190.2 | -157.7 | -5.9 |
| 3B (exp.) | 190 | -120.4 | +112 | 0.31 | -193.7 | -159.0 | -8.3 |
| 3 (theo.) | — | -84.4 | +105 | 0.35 | -155.4 | -118.3 | 20.4 |

The following convention is employed for values presented in Table S1: the principal components of the CSA tensor are δ_{xx} , δ_{yy} and δ_{zz} , with $|\delta_{\text{zz}} - \delta_{\text{iso}}| \geq |\delta_{\text{xx}} - \delta_{\text{iso}}| \geq |\delta_{\text{yy}} - \delta_{\text{iso}}|$; the

isotropic chemical shift is $\delta_{\text{iso}} = \frac{1}{3}(\delta_{xx} + \delta_{yy} + \delta_{zz})$, the anisotropy is $\delta_{\text{aniso}} = \delta_{zz} - \delta_{\text{iso}}$, and the asymmetry is $\eta_{\text{asym}} = \frac{\delta_{yy} - \delta_{xx}}{\delta_{\text{aniso}}}$, where $\eta_{\text{asym}} = 0$ is axially symmetric. The CP contact time yielding maximum intensity is denoted τ_{CP} . The ^{29}Si chemical shift of 3-(trimethylsilyl)-propanoic acid, calculated using DFT using the same procedure and basis set as for compounds **2** and **3**, was used as a reference.

S3. Single crystal X-ray analysis and DFT geometry optimizations:

Crystals for compounds **2–4** were measured on a Bruker three-circle diffractometer equipped with a SMART 6000 CCD area detector and a CuK α rotating anode. Details of Crystal data and structure refinement parameters for compounds **2–4** are given in table S2. Integrations were performed with SAINT.^(S4) Intensity data for all compounds were corrected for absorption and scaled with SADABS.^(S5) Structures were solved by direct methods and initially refined by full-matrix least-squares methods on F^2 with the program SHELXL-97,^(S6) utilizing anisotropic displacement parameters for non-hydrogen atoms. The structural model was improved [0.46 % in R1 for **2**, 0.45 % in R1 for **3** and 0.74% for **4**] by a subsequent refinement with non-spherical scattering factors,^(S7) which was initiated by converged IAM parameter values. The scattering-factor model used in this refinement was based on the Hansen and Coppens multipole formalism.^(S8) Instead of adjusting the respective multipole parameters to the experimental data, which requires Bragg data to a high resolution, multipole parameters were predicted from theoretical geometry optimizations on each whole molecule, using the density functional theory (DFT) functional B3LYP and 6-31 g* as the basis set. The whole-molecule approach was developed and successfully applied for silylene complexes before.^(S9) Prior to refinement with XDLSM as part of the XD suite,^(S10) input files were processed with the program InvariomTool.^(S11) The criterion for observed reflections was [$I > 3\sigma(I)$].

Table S2. Crystal and structure refinement parameters for compounds **2–4**

| Parameters | 2. n-hexane | 3. toluene | 4. toluene |
|--|--|---|---|
| Empirical formula | C ₆₀ H ₈₈ Cl ₂ N ₄ Si | C ₄₆ H ₅₄ Cl ₂ N ₂ Si _{0.89} | C ₄₆ H ₅₂ Cl ₂ GeN ₂ |
| Formula Weight | 964.33 | 730.74 | 776.39 |
| Crystal system | orthorhombic | monoclinic | monoclinic |
| Space group | <i>P</i> 2 ₁ 2 ₁ 2 ₁ | <i>C</i> 2/c | <i>P</i> 2 ₁ /n |
| Unit cell dimensions | <i>a</i> = 12.9849(3) Å <i>b</i> = 20.5346(4) Å <i>c</i> = 21.2339(4) Å β = 90.00 ° | <i>a</i> = 39.8670(9) Å <i>b</i> = 12.0678(3) Å <i>c</i> = 19.2296(4) Å β = 116.786(1) ° | <i>a</i> = 10.2536(2) Å <i>b</i> = 20.0665(4) Å <i>c</i> = 20.2533(4) Å β = 101.151(1) ° |
| Volume | 5661.8(2) Å ³ | 8258.8(3) Å ³ | 4088.52(14) Å ³ |
| Z | 4 | 8 | 4 |
| Density (calcd) | 1.131 g/cm ³ | 1.175 g/cm ³ | 1.261 g/cm ³ |
| Absorption coefficient | 1.526 mm ⁻¹ | 1.902 mm ⁻¹ | 2.464 mm ⁻¹ |
| <i>F</i> (000) | 2096 | 3123 | 1632 |
| Crystal size | 0.11 x 0.14 x 0.18 mm | 0.01 x 0.01 x 0.06 mm | 0.03 x 0.05 x 0.08 mm |
| θ range for data collection | 3.0 to 70.1° | 2.5 to 73.6° | 3.1 to 73.6° |
| Limiting indices | -15 ≤ <i>h</i> ≤ 15, -24 ≤ <i>k</i> ≤ 24, -25 ≤ <i>l</i> ≤ 22 | -49 ≤ <i>h</i> ≤ 47, -14 ≤ <i>k</i> ≤ 14, -21 ≤ <i>l</i> ≤ 23 | -12 ≤ <i>h</i> ≤ 12, -24 ≤ <i>k</i> ≤ 24, -25 ≤ <i>l</i> ≤ 24 |
| Reflections collected | 126973 | 86638 | 130553 |
| Independent reflections | 10640 (<i>R</i> _{int} = 0.043) | 8250 (<i>R</i> _{int} = 0.044) | 8062 (<i>R</i> _{int} = 0.048) |
| Completeness | 0.991 | 0.993 | 0.978 |
| Refinement method | Full - matrix least - squares on <i>F</i> | Full - matrix least - squares on <i>F</i> | Full - matrix least - squares on <i>F</i> |
| Data/restraints/parameters | 10476 / 0 / 626 | 7453 / 0 / 385 | 7217 / 0 / 509 |
| Goodness - of - fit on <i>F</i> ² | 3.90 | 0.97 | 1.14 |
| Final <i>R</i> indices [<i>I</i> >3σ] | <i>R</i> 1 = 0.0309, <i>wR</i> 2 = 0.0410 | <i>R</i> 1 = 0.0559, <i>wR</i> 2 = 0.0805 | <i>R</i> 1 = 0.0410, <i>wR</i> 2 = 0.0536 |

All H-atoms including silicon bonded H1 and H2 atoms (for compounds **2** and **3**) were located in the difference Fourier map (Fig. S3c and S4c). The Si-H1 and Si-H2 bond distances [1.477 (19) and 1.461(18) Å] for compound **2** are in good agreement with theoretical predicted values (1.478 Å). However, due to disorder or large amplitude vibration in compound **3**, the Si–H bond distances [1.32(3) and 1.14(3) Å] are shorter than the theoretical value (1.470 Å,

DFT: B3LYP and 6-31 g*). These bond distances remains short even when aspherical scattering factor are used. Therefore, the Si–H bond distances for compound **3** were set to the theoretical bond lengths. Only positional and displacement parameters of non-hydrogen atoms were adjusted in the non-spherical atom refinement, so that the number of parameters was not increased in comparison to the independent atom model (IAM). Bond distances to hydrogen atoms were set to values from geometry optimization.^(S12) These aspherical atom refinements share the benefits of a conventional charge-density refinement. For all compounds, parameter precision (as indicated by parameter standard deviations) and figures of merit improve. Anisotropic displacement parameters (ADPs) become deconvoluted from electron density, and an interpretable electron density model was obtained (Fig. S3-6). Calculated deformation densities show the expected electron density accumulations in bonding regions. Valence-shell charge concentrations (VSCCs) of σ -donation can also be localized by calculating and interpreting the Laplacian of the electron density.

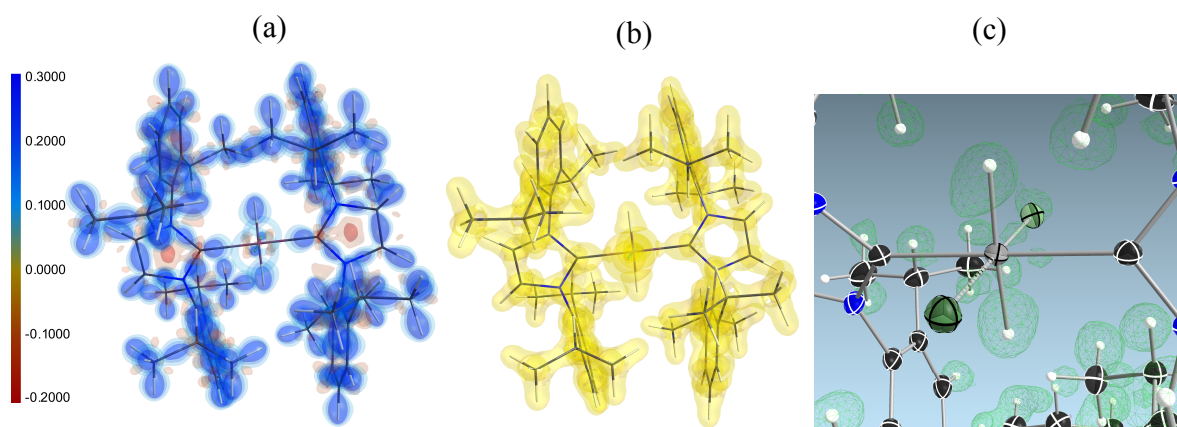


Fig. S3. (a) 3d-Deformation electron density plot^(S13) of compound **2**. (b) Isosurface plot of the Laplacian $\nabla^2 p(r)$ of the electron density of **2** from aspherical atom refinement with an isosurface value of $0.2 \text{ e}\text{\AA}^{-5}$. Anisotropic displacement parameters were omitted for clarity. The VSCCs from σ -donation are visible on the C(2)–Si bond. (c) Mash of the residual electron density without hydrogen atoms (hydrogen omit map) at $0.2 \text{ e}\text{\AA}^{-3}$ (green) and $-0.2 \text{ e}\text{\AA}^{-3}$ (red). Both hydrogen atoms at the silicon atom can be unambiguously located in the difference Fourier map

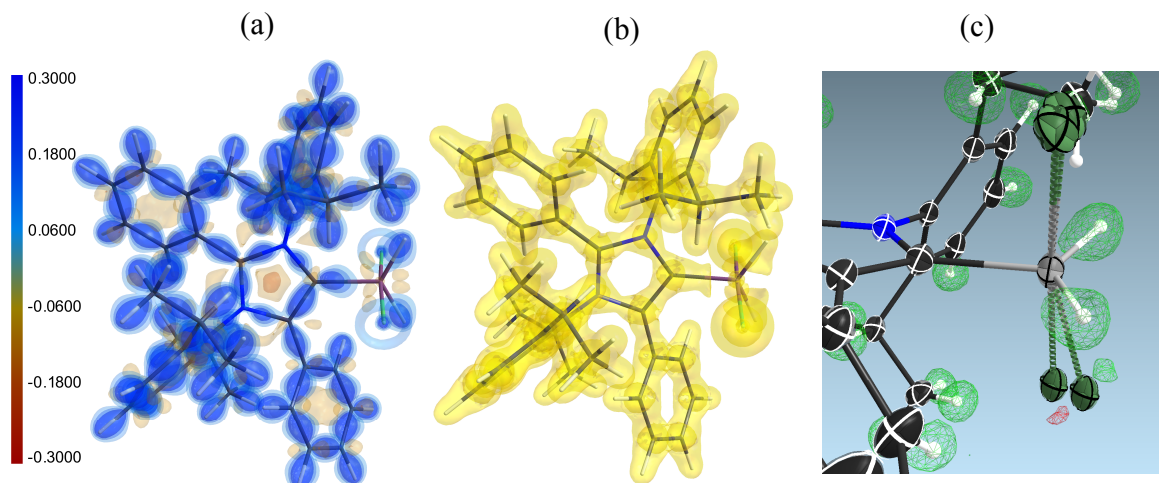


Fig. S4. (a) 3d-Deformation electron density plot^(S13) of compound 3. (b) Isosurface plot of the Laplacian $\nabla^2\rho(r)$ of the electron density of 3 from aspherical atom refinement with an isosurface value of $0.2 \text{ e}\text{\AA}^{-5}$. Anisotropic displacement parameters were omitted for clarity. The VSCCs from σ -donation are visible on the C(5)–Si bond. (c) Mash of the residual electron density without hydrogen atoms (hydrogen omit map) at $0.2 \text{ e}\text{\AA}^{-3}$ (green) and $-0.2 \text{ e}\text{\AA}^{-3}$ (red). Both hydrogen atoms at the silicon atom can be unambiguously located in the difference Fourier map

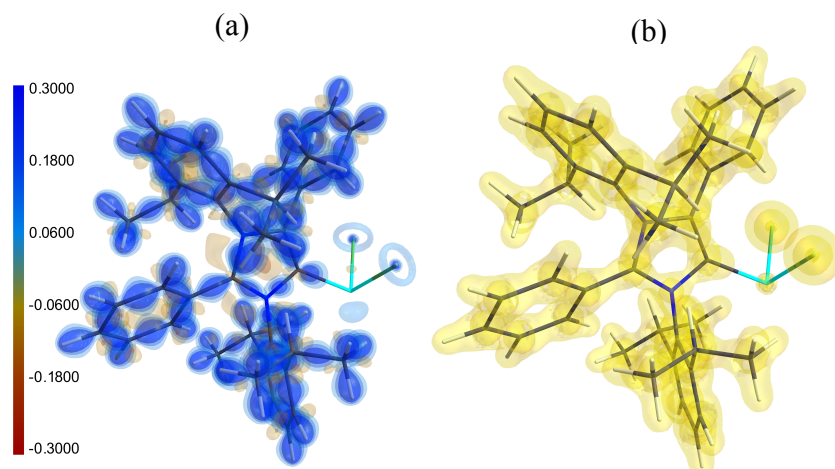


Fig. S5. (a) 3d-Deformation electron density plot^(S13) of compound 4. (b) Isosurface plot of the Laplacian $\nabla^2\rho(r)$ of the electron density of 4 from aspherical atom refinement with an isosurface value of $0.2 \text{ e}\text{\AA}^{-5}$. Anisotropic displacement parameters were omitted for clarity. The VSCCs from σ -donation are visible on the C(5)–Ge bond.

S4. References:

- (S1). E. Aldeco-Perez, A. J. Rosenthal, B. Donnadieu, P. Parameswaran, G. Frenking and G. Bertrand, *Science* 2009, **326**, 556–559.
- (S2). B.M. Fung, A.K. Khitrin, K. Ermolaev, *J. Magn. Reson.* 2000, **142**, 97–101.
- (S3). S.A. Smith, T.O. Levante, B.H. Meier, R.R. Ernst, *J. Magn. Reson. A*, 1994, **106**, 75 – 105.
- (S4). Bruker APEX2, SAINT, and SHELXTL, Bruker AXS Inc.: Madison, WI, 2009.
- (S5). G. M. Sheldrick, SADABS; University of Göttingen, Göttingen, Germany, 2009.
- (S6). G. M. Sheldrick, *Acta Crystallogr.* 2008, **A 64**, 112–122.
- (S7). B. Dittrich, C. B. Hübschle, M. Messerschmidt, R. Kalinowski, D. Girnt and P. Luger, *Acta Crystallogr.* 2005, **A 61**, 314–320.
- (S8). N. K. Hansen and P. Coppens, *Acta Crystallogr.* 1978, **A 34**, 909–921.
- (S9). R. S. Ghadwal, R. Azhakar, K. Pröpper, J. J. Holstein, B. Dittrich and H. W. Roesky, *Inorg. Chem.* 2011, **50**, 8502–8508.
- (S10). T. Koritsánszky, T. Richter, P. Macchi, A. Volkov, C. Gatti, S. Howard, P. R. Mallinson, L. Farrugia, Z. W. Su and N. K. Hansen, Freie Universität Berlin, Berlin, 2003.
- (S11). C. B. Hübschle, P. Luger and B. Dittrich, *J. Appl. Crystallogr.* 2007, **40**, 623–627.
- (S12). B. Dittrich, C. B. Hübschle, P. Luger and M. A. Spackman, *Acta Crystallogr.* 2006, **D65**, 1325–1335.
- (S13). Deformation electron density plot, which shows the difference between the total electron density (as modelled by the non-spherical scattering factors) and the independent atom model without hydrogen atoms. Deformation density represents the non-spherical part of the electron density and highlights the covalent character of most bonds. Values of the isosurfaces range from 0.3 to 0.3 eÅ⁻³ with step sizes of 0.1 eÅ⁻³, as indicated in the legend.